25 January 1963, Volume 139, Number 3552 SCIENCE

# Propagation of Air Waves from Nuclear Explosions

Nuclear explosions provide data on the relation of air-wave propagation to atmospheric structure.

William L. Donn, Richard L. Pfeffer, Maurice Ewing

When explosions occur in the atmosphere, pressure waves radiate in all directions and travel for distances that depend on the intensity of the disturbance. Low-frequency pressure waves generated by large thermonuclear explosions can be readily detected days after the time of detonation. Waves from recent very large nuclear explosions were still detectable after having made at least three circuits of the earth.

The only known natural phenomena comparable in magnitude to these great nuclear explosions are the disturbances associated with the Krakatoa eruption of 1883 (*1*) and the impact of the great Siberian meteorite of 1910 (*2*). The world-wide atmospheric data from these early natural events have added considerably to our knowledge of wave propagation, but records obtained through the very sensitive recorders of atmospheric pressure which have monitored the controlled nuclear explosions have given much greater detail regarding the nature of the waves that travel from explosions. This in turn has stimulated further theoretical investigation of the physical principles and mechanisms involved. Thus, a new tool has been provided for studying the means by which wave propagation is controlled by the structure of the atmosphere.

Because these waves travel under the joint influence of the acoustic properties of the atmosphere and gravity, they are called acoustic-gravity waves, in distinction to pure acoustic waves (sound waves) and pure gravity waves. Although these waves are not audible, because of their low frequency or long period (their period is from about 0.5 minute to 20 minutes), they are referred to as "acoustic" because the mechanism of their propagation and the parameters that control it are in part the same as the mechanism and parameters for the higher-frequency sound waves.

Initially, a spherical wave is generated by a disturbance in the atmosphere. However, this wave is soon modified, by the layered nature of the atmosphere, to a cylindrical wave that travels away from the source at approximately the speed of sound in air. The impulse at the source consists of components of many different wavelengths, or wave periods. For waves of this type the atmosphere is a dispersive medium —that is, waves of different period travel at different speeds. Generally, the dispersion for these waves is such that the speed is greatest for the longer waves and decreases with decreasing wavelength or period so that, at a distance from the source, the initial impulse becomes resolved into a train of waves of decreasing period.

As we explain in detail in a later section, the nature of the dispersion, as well as other aspects of the waves, is controlled largely by the thermal structure of the atmosphere. It is interesting to note that earthquakes are the natural analogs of atmospheric explosions. Our knowledge of the dispersion of earthquake surface waves that results from the layered structure of the earth's crust and mantle has become one of the most powerful tools in the investigation of the earth's interior. The procedure in earthquake-wave study has been to compare the dispersion (expressed as curves of wave velocity plotted against period) found from observation of surface waves with the dispersion calculated from theoretical models of the earth in which the major variables are the elastic properties and the thickness of the terrestrial layers.

## Instrumentation

The atmospheric acoustic-gravity waves produced by large explosions have been detected at great distances from the source by sensitive microbarovariographs. These instruments are designed to record only the variations in pressure, not the absolute pressure. By keeping the time constants sufficiently small, the large diurnal pressure changes can be suppressed and the much weaker short-period pressure changes (periods of the order of minutes) can be given considerable magnification. At least a half-dozen types of such instruments have been described as giving good operational results. The Lamont system, in which a "U-tube" manometer is used as the sensor, was developed to meet the need for a portable, easily operated unit for field use in the International Geophysical Year.

The manometer in the Lamont system measures the pressure difference between a thermally insulated reference

Dr. Donn is professor of geology at Brooklyn College and research associate of the Lamont Geological Observatory of Columbia University. Dr. Pfeffer is assistant professor of meteorology at Columbia University and senior research scientist at the Lamont Observatory. Dr. Ewing is professor of geophysics at Columbia University and director of the Lamont Geological Observatory.

volume and the atmosphere. It contains a very stable fluid (dioctyl sebacate), which is very low in thermal expansion, creep, and vapor pressure. Fluctuations of the level of liquid in the open end of the U are sensed by a float which is coupled to a moving coil in a differential transformer whose 60-cycle output is directly proportional in magnitude to the changes in level of the liquid. Amplification and demodulation of the signal gives a sensitivity of about 0.035 millibar (35 dynes/cm$^2$) per centimeter of scale deflection for a step displacement. A direct-current postamplifier can give an increased sensitivity of about 0.001 millibar (1 dyne/cm$^2$) per centimeter of scale deflection. Broad-band recording is best accomplished at the lower sensitivity. At this sensitivity the time constants of the transducer are controlled by an adjustable slow leak between the closed end of the manometer and the thermally insulated reference volume. At the higher sensitivity the necessary narrow passband requires additional electronic filtering. The Lamont pressure transducer is illustrated schematically in Fig. 1, where its electric analog is also shown, together with a block diagram of the entire system.

The original Lamont program, which was directed toward the study of slowly moving atmospheric gravity waves (waves which travel on density discontinuities such as frontal or other inversion surfaces), involved the installation of an array of four instruments from which signals are telemetered to the laboratory. Knowing the time of arrival of a wave at each station, we can compute the speed and direction of the wave. In Fig. 2 a comparison is given between the slowly moving gravity waves (about 20 m/sec) from the southeast and the fast acoustic-gravity waves from the Soviet multimegaton nuclear explosion of 5 August 1962 in Novaya Zemlya. The waves from the nuclear explosions differ from the slower gravity waves in that the former are dispersive, with period decreasing from left to right in the record, and that they arrive at the several recording stations at almost the same time.

In addition to the data obtained from the widespread network of microbarovariographs maintained by Lamont and institutions from other countries, useful records have been provided by Lamont's global array of long-period seismographs. These sensitive instruments, when no compensation, or only partial compensation, has been made for changes in atmospheric pressure, act as fairly good microbarovariographs.

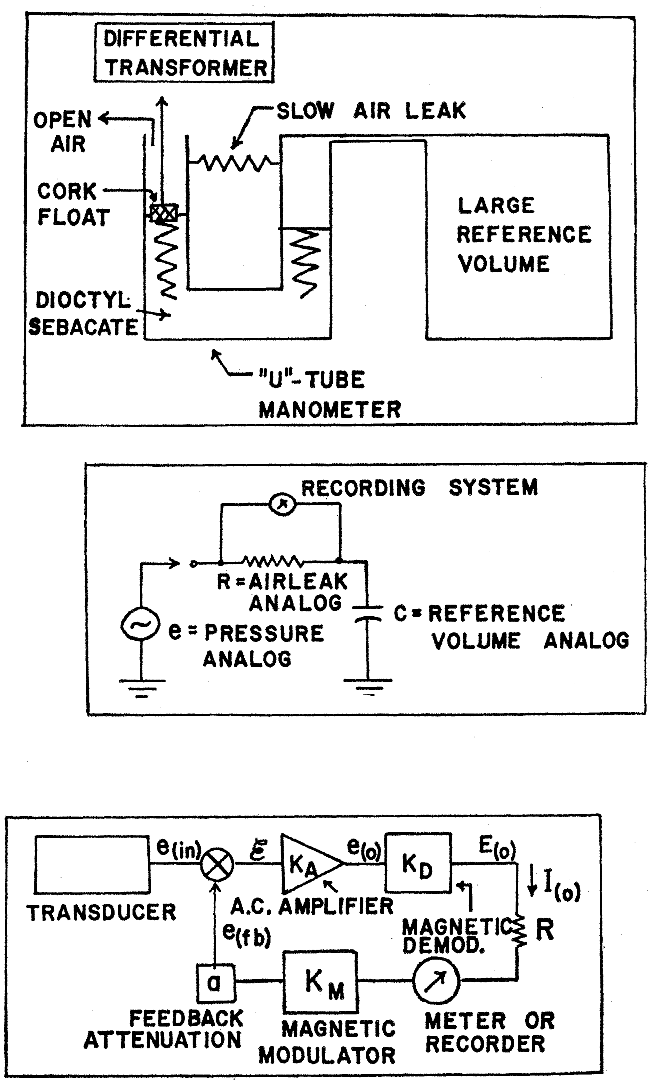


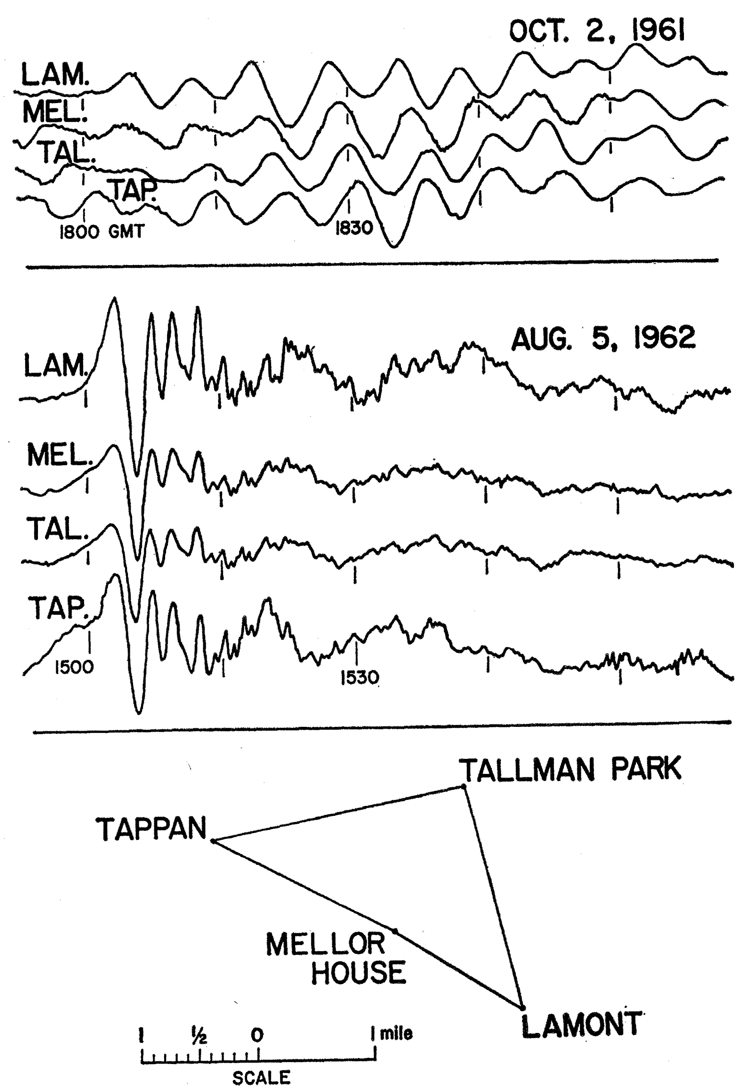


Fig. 1 (left). The Lamont microbarovariograph system: a schematic drawing of the pressure transducer and its electric analog and a block diagram of the entire system. Fig. 2 (right). A comparison of multipartite records of acoustic-gravity waves of relatively high velocity from the Soviet nuclear explosion of 5 August 1962 in Novaya Zemlya and of slower internal gravity waves of local origin (2 October 1961). The drawing at bottom illustrates the multipartite instrument array.

## Waves from Nuclear Explosions

R. Yamamoto was the first (*3*) to describe and interpret pressure waves recorded in Japan from U.S. and Soviet nuclear explosions in the Marshall Islands and Siberia, respectively. The Lamont program to investigate phenomena associated with small-pressure fluctuations, which was begun initially as part of a global seismic program, gained considerable impetus with the beginning of the IGY. Two of us (W.L.D. and M.E.) (*4, 5*) recently gave detailed descriptions and analyses of more than 36 sets of records of explosions, beginning with the early hydrogen-bomb explosions of 1952. Analysis of records from large Soviet and U.S. explosions of 1961 and 1962 is still under way. Owing to improvements in instrumentation as well as to the high yield, this series has provided extremely valuable data.

A number of recordings made by Lamont and other institutions for the 57-megaton Soviet nuclear tests of 30 October 1961 are shown in Fig. 3, together with some records produced by the explosions of 23 October 1961 and 5 August 1962, both of which were believed to have yields of about 30 megatons. All of the records shown are from the Lamont network except for those from Foulness, Stockholm, and Kyoto; of those three, the first two were copied from the literature (*6*), the third was generously furnished by R. Yamamoto. The locations of the stations, together with data on explosion sources and origin times for all the records shown in Figs. 3 and 4, are given in Tables 1 and 2.

In Fig. 3 the pressure traces designated $A_1$ represent the direct wave train; $A_2$ represents the waves that have traveled through the source antipodes, and $A_3$, the direct waves after a complete global passage. Although waves of still higher orders have also been detected, particularly from the 30 October explosion, they are not reproduced here. The $A_1$ traces begin with a strong increase in pressure; this is followed by a sharper decrease in pressure. Where waves of orders greater than $A_1$ have been detected, a noticeable phase change has been seen to occur with each circumferential passage. (The arrow shown with each trace indicates increasing pressure.) An analysis of this effect for seismic surface waves has already been given by Brune, Nafe, and Alsop (*7*). The short-period "chop" on some of the records results from local turbulence. The "stretching" of the wave trains from dispersion over long distances is very evident when we compare the $A_1$, $A_2$, and $A_3$ traces for the tests of 30 October 1961 recorded at Palisades. The appearance of the $A_3$ trace is especially clear, owing to the absence of wind noise.

In general, the first several wave cycles on all records (the waves of maximum amplitude) show normal or direct dispersion—that is, there is a decrease in wave period with time, indicating a decrease in group velocity with decrease in period. Following, and often superimposed on, the initially observed dispersive wave train are one or more groups of waves of nearly constant period. As we shall see later, these wave groups are the result of different modes of propagation (analogous to harmonics or overtones in music) which result from differences in wave paths through the layered atmosphere.

The records from these large explosions suggested to Donn and Ewing (*5*) for the first time the possibility that a long-period train of waves showing inverse dispersion (period increases with time) is present. The dashed, overprinted lines on some of the records in Figs. 3 and 4 show where these waves seem to occur. Figure 4 shows pressure traces recorded at the Lamont installation in the Honolulu Observatory (Ewa Beach) of the U.S. Coast and Geodetic Observatory during the recent U.S. tests in the vicinity of Christmas Island, near the Central Pacific Ocean. Because of the relatively short distance (2135 km) and the low level of background noise, three tests in the intermediate-range yield (Atomic Energy Commission designation, 20 to 999 kilotons) were recorded (traces for tests of 9, 10, and 12 June).

From initial arrival times for waves of the first three orders from the explosion of 30 October 1961, we determined the velocity of the energy front to be 324 meters per second. This value is computed from the slope of the straight line in Fig. 5, which is obtained

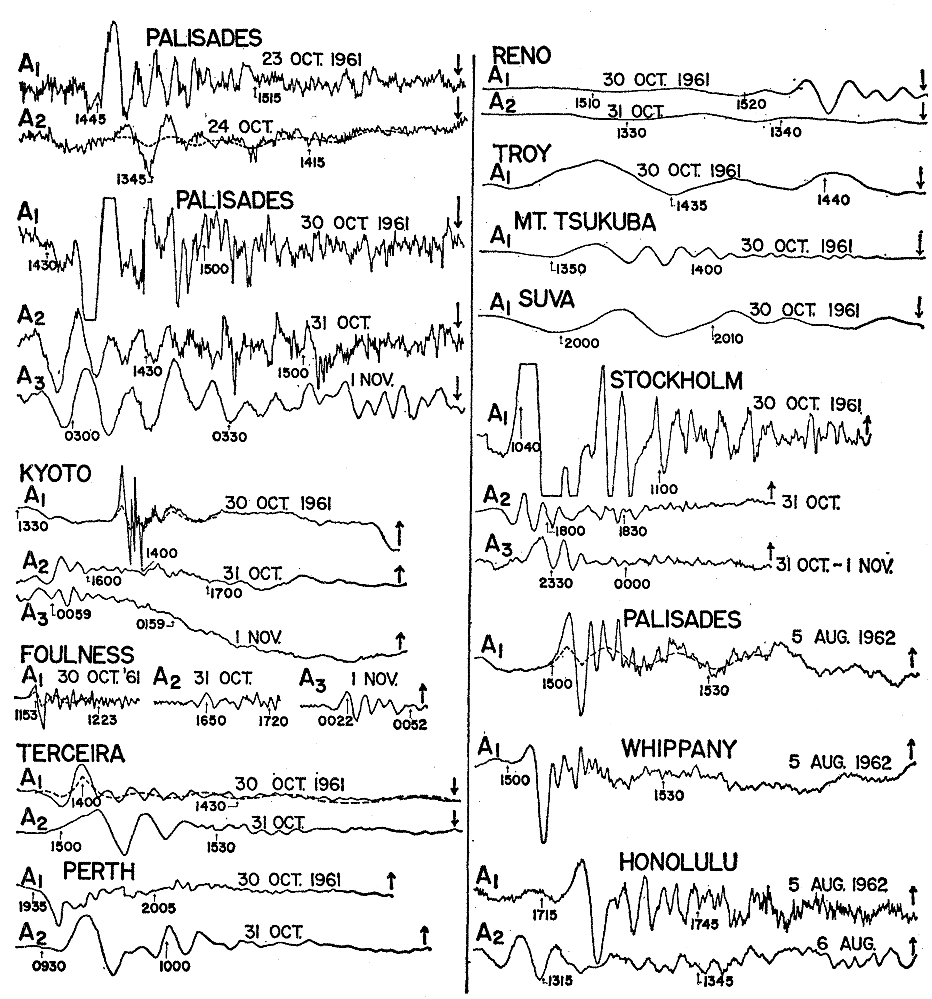


Fig. 3. Atmospheric-pressure records from the Soviet tests of 23 and 30 October 1961 and 5 August 1962, as recorded at numerous stations around the world.

from a plot of travel time against distance for the first arrivals. A maximum speed of 324.5 meters per second was obtained by Strachey (see 2) for the disturbance from the Krakatoa eruption, but the range of velocities computed from initial arrival times includes values as low as 301 meters per second. Because travel along circumferential paths removes much of the effects of zonal winds, it seems likely that the use of sensitive modern instruments, with more open time scales, now permits better detection of the first energy arrival than was possible in earlier observations. In order to determine phase velocities experimentally, a large tripartite net, involving stations at Palisades (N.Y.), Poughkeepsie (N.Y.), and Whippany (N.J.), has been set up (*8*).

**Wave Dispersion**

The investigation of the propagation of dispersive waves in layered media involves comparison of the observed wave dispersion with the theoretical dispersion calculated from various atmospheric models, because dispersion is determined by the thermal or velocity structure along the wave path. Dispersion can be studied by means of graphs of the velocity plotted against the period of the dispersive wave groups. When the location and time of origin of the source are known, measurements of wave arrival time on the records provide the basis for a rough calculation of the dispersion curves [by the method of Ewing and Press (*9*)]. These curves, determined visually for the initial large-amplitude wave train, provide valuable information quite rapidly. Dispersion curves with greater resolution in period or time can be obtained through spectrum analysis of the wave records by analog or digital computers, as will be discussed later.

Examples of empirical dispersion data from Donn and Ewing (*5*) are given in Fig. 6 for $A_1$ records and in Fig. 7 for $A_2$ and $A_3$ records from the Soviet test of 30 October 1961. Figure 6 includes an additional set of data, for Perth, Australia, for 23 October 1961. The points in these graphs are connected by continuous lines to indicate data from a single station, not dispersion of a single mode. According to Fig. 6, there is a velocity spread of 25 to 30 meters per second for waves of a particular period. Much of this can be accounted for by the differences in winds along different azimuths. The "winds-aloft" data for 1200 hours, Greenwich Mean Time on 30 October 1961 indicate that Terceira and Foulness were up-wind from the source, and that there was an opposing component of about 20 to 30 knots (10 to 15 m/sec). Stations in the United States are on azimuths for which winds were nearly, but not quite, normal to the wave paths. A slight up-wind component existed. Wind data for the critical area from the source to Suva and Japan are not available, but these stations should have been down-wind from the source, and thus one would expect the velocities recorded at them to be somewhat above the average. A similar wind effect has been reported by Yamamoto (*10*) for waves received in Japan from U.S. nuclear explosions in the Marshall Islands and from Soviet tests in Siberia, respectively. Differences in the mean temperature along the various paths can also account for such effects.

As discussed by Pfeffer and Zarichny (*11*), the temperature of the more tenuous upper air, as well as the height of the tropopause, may be very important in determining the details of the

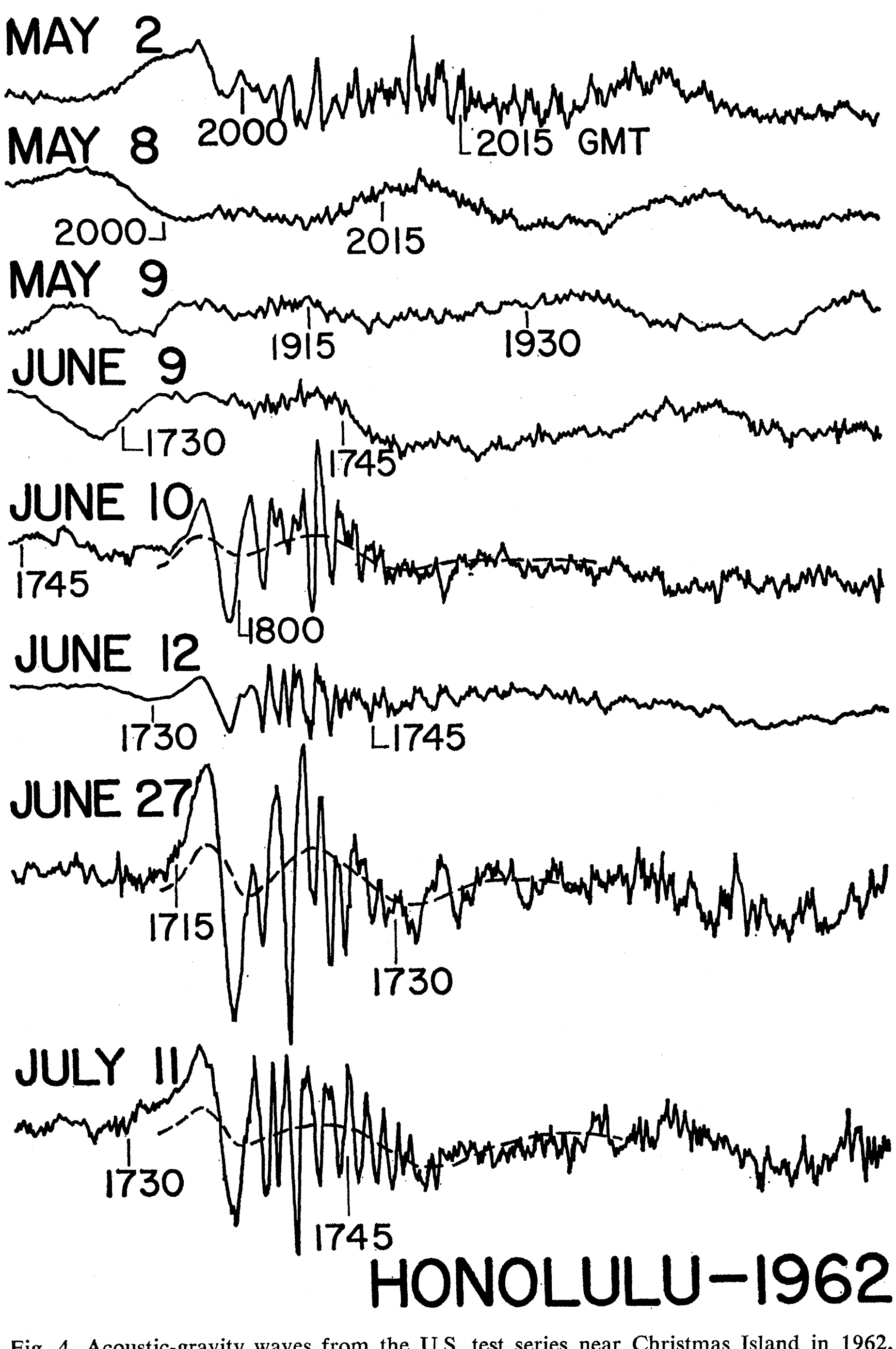


Fig. 4. Acoustic-gravity waves from the U.S. test series near Christmas Island in 1962, as recorded at the U.S. Coast and Geodetic Seismic Observatory, Ewa Beach, Honolulu.

dispersion curves. Thus, the length of ray segments in different climatic zones and in the dark and the illuminated hemispheres must also be of significance. It is interesting to note that the data for Perth, Australia, in Fig. 6 (from the test of 23 October 1961), which lie near the upper middle zone of the velocity spread, are from a station which was recording waves that had followed a nearly meridional path from the source, the zonal wind and mean temperature effects thus being minimal.

Support for this interpretation of the differences in position and shape of the $A_1$ curves is given by the data for waves of higher orders (Fig. 7). The dispersion data for these waves should more nearly reflect global average conditions. Note that the empirical curve for the $A_1$ waves for Perth (test of 23 October 1961) would be central in this group, in support of the statement that zonal wind and temperature variations would be minimal in the path these waves followed. As may be seen, the four curves of Fig. 7 are nearly identical in slope and lie within the range 300 to 315 meters per second. The low position of the curve for the $A_2$ waves at Perth probably results from wave passage through the low-temperature atmosphere of both polar regions.

Variations in wind velocity with altitude could also introduce a dispersion effect. Thus, the shape and position of observed dispersion curves may depend upon the wind as well as the temperature distribution in the atmosphere. Distortion of the curves by wind distribution has not been considered here.

The assumed inversely dispersed wave trains indicated (Fig. 3) by the dashed lines in the records of 30 October 1961 produce the long-period branches of the curves in Fig. 6. If this is a proper interpretation of the data, it indicates that a maximum for group velocity occurs at a time corresponding to the point on the record where the wave trains of normal and inverse dispersion merge into a single nondispersive wave or "Airy phase."

## Theory

By solving the appropriate hydrodynamic equations it should be possible to predict theoretically the observed properties of the waves that have been described and to gain an understanding of the mechanisms by which the waves propagate. We cannot, of course, solve

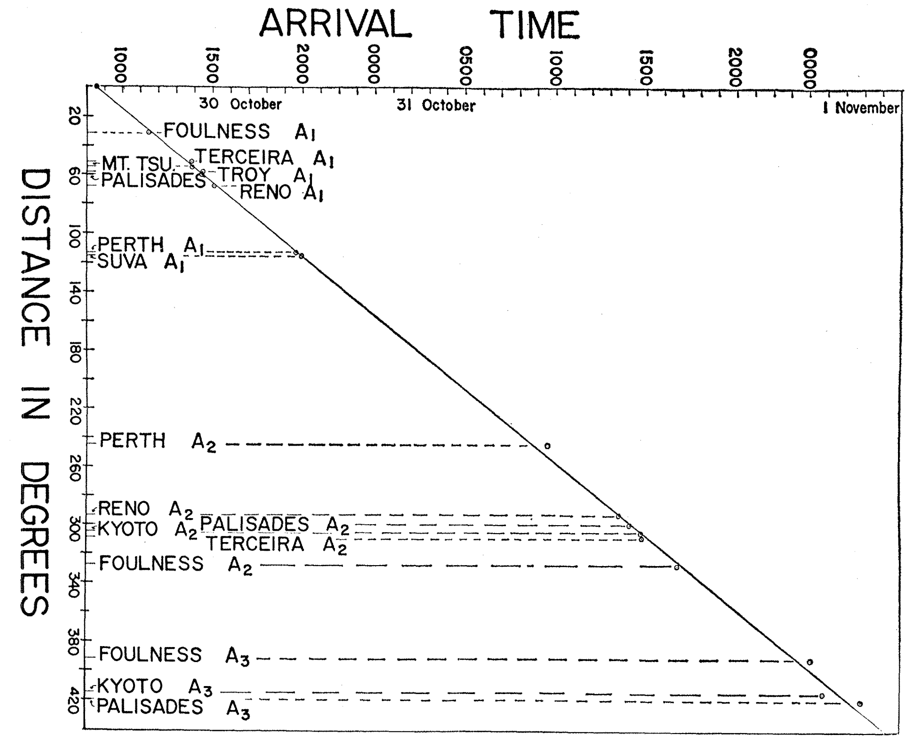


Fig. 5. Graph of arrival times for the energy front from the explosion of 30 October 1961.

Table 1. Location and origin times for Soviet explosions of 1961 and 1962, location of stations where pressure waves were recorded, and times of arrival of the wave front (see Fig. 3). All times are GMT.

| Explosion: Date, hour, place | Recording station | Wave order | Arrival time |
|---|---|---|---|
| 23 Oct. 1961; 0831 (73°24′N, 54°54′E) | Palisades, New York (41°00′N, 73°54′W) | $A_1$<br>$A_2$ | 23 Oct.; 1443<br>24 Oct.; 1335 |
| 30 Oct. 1961; 0834 (74°42′N, 54°54′E) | Palisades, New York (41°00′N, 73°54′W) | $A_1$<br>$A_2$<br>$A_3$ | 30 Oct.; 1436<br>31 Oct.; 1405<br>1 Nov.; 0254 |
| 30 Oct. 1961; 0834 (74°42′N, 54°54′E) | Kyoto, Japan (35°01′N, 135°44′E) | $A_1$<br>$A_2$<br>$A_3$ | 30 Oct.; 1353<br>31 Oct.; 1534<br>1 Nov.; 0043 |
| 30 Oct. 1961; 0834 (74°42′N, 54°54′E) | Foulness, England (51°30′N, 00°50′E) | $A_1$<br>$A_2$<br>$A_3$ | 30 Oct.; 1126<br>31 Oct.; 1624<br>1 Nov.; 0006 |
| 30 Oct. 1961; 0834 (74°42′N, 54°54′E) | Terceira, Azores (38°43′N, 27°13′W) | $A_1$<br>$A_2$ | 30 Oct.; 1356<br>31 Oct.; 1440 |
| 30 Oct. 1961; 0834 (74°42′N, 54°54′E) | Perth, Australia (31°57′S, 115°50′E) | $A_1$<br>$A_2$ | 30 Oct.; 1935<br>31 Oct.; 0930 |
| 30 Oct. 1961; 0834 (74°42′N, 54°54′E) | Reno, Nevada (39°32′N, 119°48′W) | $A_1$<br>$A_2$ | 30 Oct.; 1500<br>31 Oct.; 1327 |
| 30 Oct. 1961; 0834 (74°42′N, 54°54′E) | Troy, New York (42°43′N, 73°43′W) | $A_1$ | 30 Oct.; 1430 |
| 30 Oct. 1961; 0834 (74°42′N, 54°54′E) | Mt. Tsukuba, Japan (36°12′N, 140°06′E) | $A_1$ | 30 Oct.; 1350 |
| 30 Oct. 1961; 0834 (74°42′N, 54°54′E) | Suva, Fiji (18°09′S, 178°26′E) | $A_1$ | 30 Oct.; 1956 |
| 30 Oct. 1961; 0834 (74°42′N, 54°54′E) | Stockholm, Sweden (59°20′N, 18°06′E) | $A_1$<br>$A_2$<br>$A_3$ | 30 Oct.; 1037<br>31 Oct.; 1733<br>31 Oct.; 2303 |
| 5 Aug. 1962; 0909 (74°12′N, 52°30′E) | Palisades, New York (41°00′N, 73°54′W) | $A_1$ | 5 Aug.; 1459 |
| 5 Aug. 1962; 0909 (74°12′N, 52°30′E) | Whippany, New Jersey (40°49′N, 74°25′W) | $A_1$ | 5 Aug.; 1501 |
| 5 Aug. 1962; 0909 (74°12′N, 52°30′E) | Honolulu, Hawaii (21°18′N, 158°06′W) | $A_1$<br>$A_2$ | 5 Aug.; 1718<br>6 Aug.; 1239 |

the complete system of nonlinear equations governing atmospheric motions, even with modern electronic computers. However, by confining our attention to certain aspects of the problem we can reduce the equations to a simplified form in which they can be solved to give the basic information we desire. In the present case, we wish to answer three questions, as follows. (i) In an atmosphere with a prescribed temperature structure, what modes of wave propagation can exist? (ii) How are the velocity-period relationships associated with these modes controlled by the temperature structure of the atmosphere? (iii) Which of the possible modes of wave propagation will actually be excited by an explosion of a given magnitude at a given elevation?

The answers to questions i and ii can be obtained by reducing the equations to a homogeneous form and by solving to determine the free periods of oscillation of the atmosphere. Answering question iii however, requires consideration of the nonhomogeneous problem and computation of a Green's function, or excitation function, for the problem. In this article we confine our attention to the free-wave theory and compare some of the results obtained from the theory with results derived from the observed wave records. The considerations that follow enable us to reduce the governing equations to a form in which they can be solved.

At great distances from the source, the waves produced by large explosions propagate as small-amplitude perturbations superimposed upon an equilibrium state of the atmosphere. Thus, we may linearize the equations. In the equilibrium state, the atmosphere is, to a first approximation, at rest and in hydrostatic balance. The equilibrium pressure and density vary mainly along the vertical, whereas the perturbation pressure, vertical velocity, and velocity divergence must be treated as functions of distance from the source, time after the explosion, and elevation. The observed wave periods are short enough (that is, below 20 minutes) for us to neglect the rotation of the earth, but we must retain the acceleration of gravity in our equations. Since the wavelengths associated with these periods are short in comparison with the radius of the earth, the earth may be treated as being flat. As a first approximation we may also disregard the effects of heating and viscosity. In addition, since we are interested in free oscillations traveling radially outward from a point source in a shallow, layered atmosphere, we may, for all practical purposes, regard the waves at great distances from the explosion as being symmetrical about a vertical axis through the source. As a final simplification, we may neglect the azimuthal component of the motion about this axis. With these assumptions, the hydrodynamical equations can be reduced to a system of linear ordinary differential equations which can be solved by analytical methods for extremely simple models of the atmospheric structure and by numerical methods for more complex, but more realistic, models. The derivation and form of the equations are given by Lamb (*12*). It should be remarked that the general theory and procedures for solving the equations are applicable also to the study of free oscillations of atmospheres of other planets.

In order to solve the problem it is necessary to have some knowledge of the vertical temperature structure of the atmosphere, the most influential of the factors that determine the speed of propagation of the waves. In the earth's atmosphere, and doubtless also in the atmospheres of the other planets, the vertical temperature structure varies with both time and space. The problem is complicated further by the fact that present determinations of even the mean structure of the atmosphere, particularly at the high altitudes (above 100 km), must be regarded as only preliminary estimates. Nevertheless, we can make a beginning by using the latest estimates from rocket and satellite measurements as the basis for our calculations. It should be noted, however that comparison of observational data with the results of theoretical calculations can be used conversely as a tool to aid in the determination of the structure of the atmosphere.

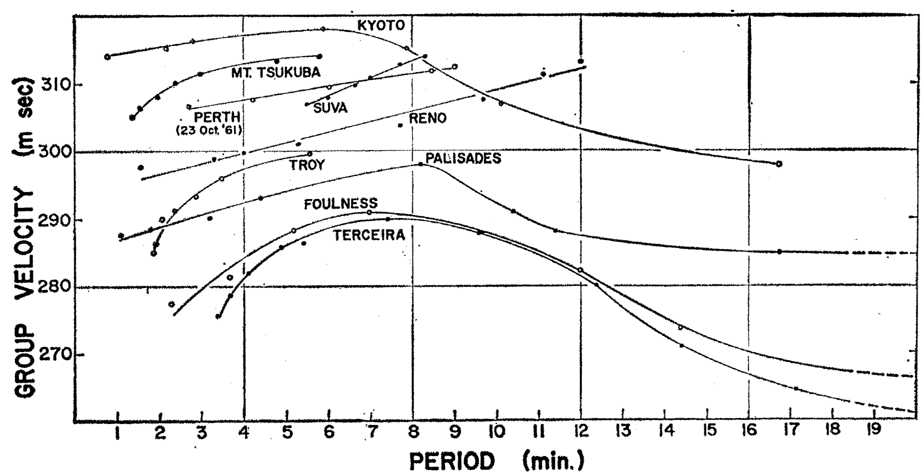


Fig. 6. Empirical dispersion curves for selected $A_1$ pressure waves.

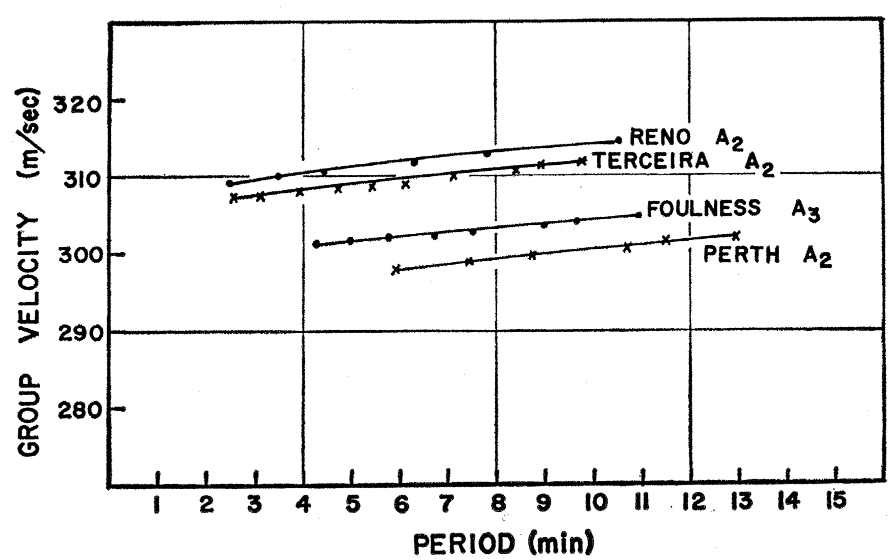


Fig. 7. Empirical dispersion curves for selected $A_2$ and $A_3$ pressure waves.

As noted earlier this has proved to be an extremely powerful tool in seismology for investigating the structure of the solid earth.

A recent estimate for the mean temperature structure of the earth's atmosphere, as agreed upon by the International Committee on Space Research (COSPAR) (*13*) is shown by the solid curve in Fig. 8. At elevations up to about 30 kilometers the temperature is known from direct measurements by instruments carried on sounding balloons. Above this elevation it can be calculated from the hydrostatic equation if the density is known. Since the end of World War II rocket measurements of density at altitudes up to nearly 200 kilometers have become available. More recently, average densities at higher altitudes have been deduced from information concerning the drag on artificial satellites. As noted by Sissenwine, Dubin, and Wexler (*14*), the temperature structure from about 30 to 90 kilometers is regarded as tentative and the structure above 90 kilometers is considered speculative.

*Two-layer models.* Inasmuch as almost 90 percent of the mass of the atmosphere lies below an altitude of only 15 kilometers, the details of the temperature distribution above this elevation are of little importance in many geophysical problems. The atmosphere up to 15 kilometers can be considered to consist of two layers—a troposphere, with a constant lapse rate of temperature, and an isothermal stratosphere, which is colder than the troposphere. Even when we neglect the details of the temperature structure above a given level in the atmosphere, we must still regard the last isothermal layer as one which extends upward to an infinite altitude, and we must consider the density of the air as decreasing exponentially with elevation within each layer. Studies of free oscillations of such a two-layer atmosphere were conducted by Pekeris (*15*) and Scorer (*16*) before many of the details shown in Fig. 8 were known. The theory shows that the waves are dispersive, but it predicts that waves with periods of less than about 2 minutes must be attenuated before they can be propagated over great distances. Since the stratosphere is assumed to be infinitely deep and to have a lower temperature than the troposphere, short-period waves refracted into the stratosphere would suffer no further refraction or reflection and would, therefore, propagate toward infinite altitudes. Although not explicitly taken into account in the theory, heat conduction and molecular viscosity are assumed to attenuate these waves. Actually, however, the presence of these waves on the microbarograms after large nuclear explosions (see, for example, Fig. 3) reveals that such waves travel around the earth with comparatively little attenuation. In the real atmosphere, the cold stratosphere is confined between two warmer layers—the troposphere below and the ozonosphere above. It is known that a cold (low-velocity) layer bounded by warmer (higher-velocity) layers above and below should serve as a "sound channel" in which the short-period acoustic waves become "trapped" as they travel around the earth. Since waves which are confined to a sound channel travel with very little attenuation, we should expect to find evidence of such waves on barograms located at great distances from the source of the explosions. However, the amplitude of these waves as recorded at the ground should be small, because the receiver is remote from the channel.

*Models with one sound channel.* Several investigators [Yamamoto (*17*); Hunt, Palmer, and Penney (*18*); Gazaryan (*19*); and Pfeffer (*20*)] have formulated and solved equations governing free oscillations of model atmospheres in which the stratosphere is treated as the only sound channel. According to the theory there are an infinite number of modes of propagation. If we plot the perturbation pressure as a function of altitude, we may distinguish the modes from one another by the number of times this curve crosses zero pressure. We shall define the "fundamental mode" as that mode for which the pressure curve does not

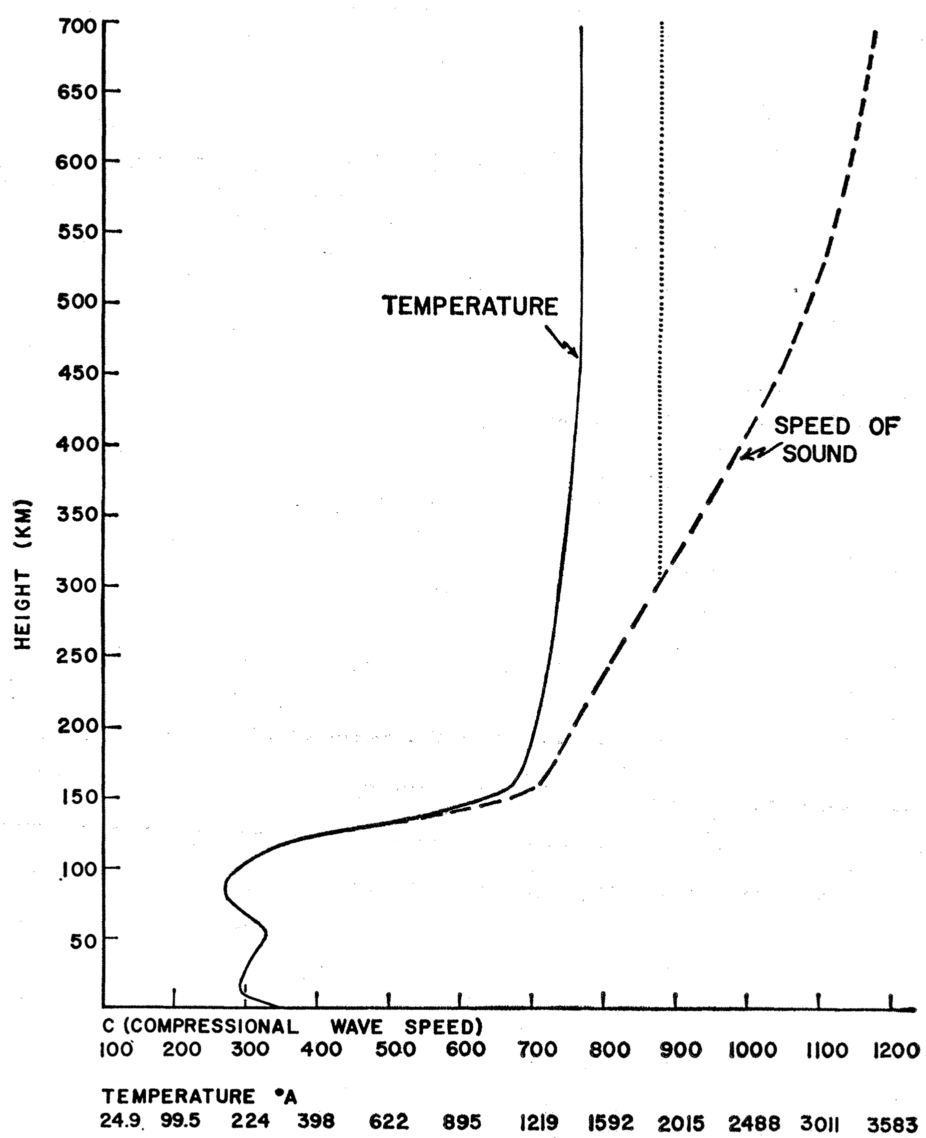


Fig. 8. Temperature and related compressional wave speed, and structure of the atmosphere. [After Kallman-Bijl *et al.* (*13*)]

cross zero at any finite elevation. Two families of higher modes have been found by Gazaryan and by Pfeffer and Zarichny. In each family the pressure curve has one zero for the first higher mode, two for the second, and an additional zero for each successive higher mode in each family. Each mode has a different velocity-period relationship. Unlike the situation with the two-layer atmospheres, there is no mode for which there is a short-period cutoff of energy. However, both families of higher modes, and often also the fundamental mode, have long-period cutoffs. That is, waves with periods greater than a certain critical value for each mode are rapidly attenuated with distance from the source.

One family of modes disappears when gravity is set at zero in the equations. These modes, which we shall refer to as the gravity modes, have *phase* velocities which increase from zero at short periods and cut off at periods greater than 5 minutes. Such velocity-period relationships are consistent with the well-known theory of gravity waves on an interface between two deep layers of fluid. For a given period of oscillation the successively higher gravity modes have successively lower phase velocities.

The other family of modes has phase velocities which approach that of the fundamental mode at the "acoustic limit" (zero period) and increase with period to cutoff points which, in every case we have studied, are below 5 minutes. At a given period the successively higher modes in this family have successively higher phase velocities.

Table 2. Origin times for explosions of the United States series of 1962 at Christmas Island (02°N, 157°30′W) and times of arrival of the wave front at Honolulu (21°18′N, 158°06′W) (see Fig. 4). All times are Greenwich Mean Time.

| Explosion: Date, hour | Arrival: Date, hour |
|---|---|
| 2 May 1962; ~1800 | 2 May; 1956 |
| 8 May 1962; ~1800 | 8 May; 2003 |
| 9 May 1962; ~1700 | 9 May; 1907 |
| 9 June 1962; ~1530 | 9 June; 1736 |
| 10 June 1962; ~1600 | 10 June; 1755 |
| 12 June 1962; ~1530 | 12 June; 1731 |
| 27 June 1962; ~1530 | 27 June; 1714 |
| 11 July 1962; ~1530 | 11 July; 1732 |

These we call the acoustic modes, although their velocity-period relationships are greatly modified by the acceleration of gravity.

The relative excitation of the various modes for explosions at different elevations in the atmosphere is being studied at the Lamont Observatory. As in other problems of this kind (for example, in seismology and in oceanography), the fundamental mode has a comparatively large excitation. It is of interest to examine first the velocity-period relationships associated with this mode.

The theoretical calculations show that for models with a single sound channel the fundamental mode displays normal dispersion (group velocity increasing with period) at periods of less than about 300 seconds, with a minimum group velocity at about 30 seconds. Pfeffer and Zarichny (*11*) showed, further, that such models can produce normal dispersion, inverse dispersion (group velocity decreasing with increasing period), or no dispersion at longer periods, depending upon the details of the temperature distribution in the uppermost tenuous layers of the atmosphere (that is, above the stratosphere). This may be seen clearly in the sample dispersion curves of Fig. 9, which are taken from the paper of these investigators. Curves *a*, *b*, and *c* give the group velocity as a function of period for the fundamental mode of propagation for the model atmospheres shown in the figure. Although the three models differ in a number of respects, it is the increasingly higher temperatures of the uppermost layers of the atmosphere that bring about the changes in the dispersion curves at the long periods as we progress from *a* to *b* to *c*.

Thus, although the density of the earth's atmosphere, which decreases exponentially with altitude, is only 0.0000004 as great at 100 kilometers as it is at sea level, the details of the atmospheric structure in the tenuous upper atmosphere have an appreciable influence on the nature of the dispersion. It follows that in order to account for the observed properties of the waves it is necessary to specify in theoretical models the structure of the very high atmosphere. It should be noted (see Fig. 8) that the atmosphere possesses two sound channels and that from about 100 to 160 kilometers there is a rapid rise of temperature with height.

*Models with two sound channels.* Calculations of the dispersion curves for model atmospheres with two sound

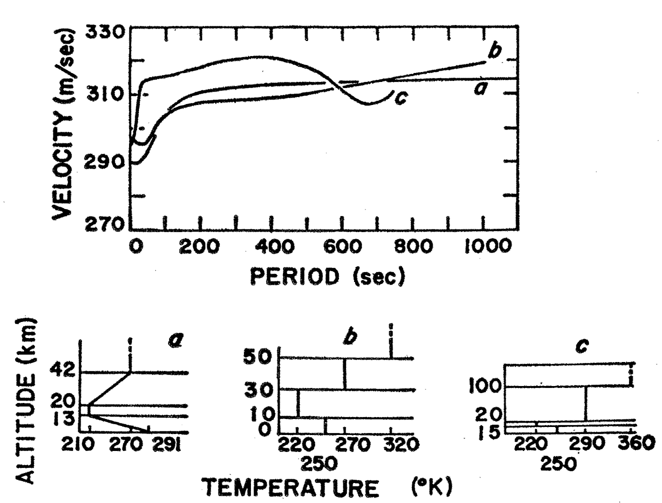


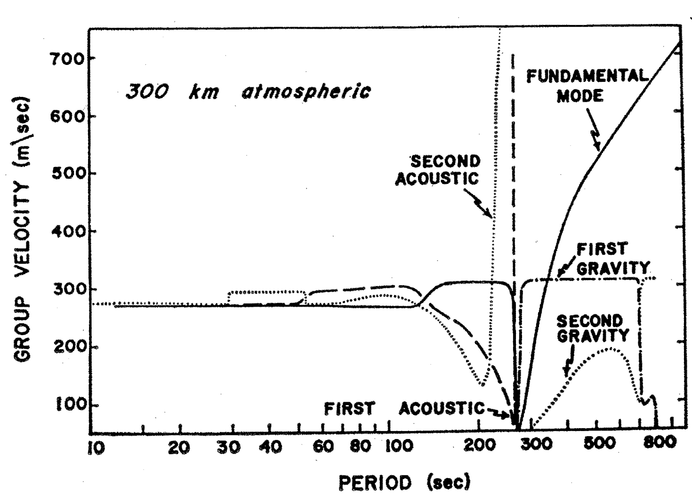


Fig. 9 (left). Theoretical curves for group velocity dispersion and related atmospheric models for a single-sound-channel atmosphere. Fig. 10 (right). Theoretical curves for group velocity dispersion for the fundamental and first two higher acoustic and gravity modes for the model of Fig. 8 (constant sound speed above 300 km). [After Pfeffer and Zarichny (*23*)] channels have been made by Gazaryan (*19*), Weston (*21*), Press and Harkrider (*22*), and Pfeffer and Zarichny (*23*). The results given in the last three papers show that it is necessary to consider more than just the fundamental mode in order to account for the observed properties of the waves. Figure 10 gives the velocity-period relationships for the fundamental and the first two higher acoustic and gravity modes as calculated by Pfeffer and Zarichny for the sound-speed distribution shown, in Fig. 8, by the solid and dashed curves up to 300 kilometers and by the dotted curve above that level. In the calculations this velocity distribution was approximated by a step function consisting of 67 constant velocity layers. The nomenclature in Fig. 10 follows that of Gazaryan and of Pfeffer and Zarichny, which is different from that of Press and Harkrider. The latter authors denote the *n*th gravity mode of Fig. 10 as the (*n*-1) gravity mode, and thus distinguish a fundamental gravity mode as well as a fundamental acoustic mode.

Before we discuss the results, a few critical remarks should be made about the problems which arise when we attempt to treat the subject of wave propagation in the very high atmosphere. First, it should be noted that the molecular weight and heat capacities of the atmosphere at constant pressure and volume vary with altitude above 100 kilometers. This means that, among other things the speed, $c$, of compression waves, which is given by

$$c = \left(\frac{\gamma RT}{m}\right)^{1/2}$$

varies with altitude even in an isothermal layer. Here $\gamma$ is the ratio of heat capacity at constant pressure to heat capacity at constant volume, $R$ is the universal gas constant, $T$ is the tempeture, and $m$ is the molecular weight. The dashed curve in Fig. 8 shows the variation of the compression speed with altitude up to 700 kilometers in the upper atmosphere. In addition, we must take into account the decrease in gravity ($g$) with height when we specify the atmospheric structure from the ground up to great heights. In the calculations on which Fig. 10 is based, the variations of $g$, $\gamma$, and $m$ were taken into account. It should be mentioned, too, that the perturbation values for density, pressure, and so on, can become very large in comparison with the mean values for these properties in the tenuous layers of the upper atmosphere, so that the linear theory is no longer valid in these regions. Furthermore, according to very recent estimates of the particle densities at high altitudes [see, for example, Harris and Priester, (*24*)], the mean free path of the molecules at 300 kilometers is already appreciably greater than wavelengths we are considering. Thus, the continuum theory is no longer valid in the very high atmosphere (*25*). However, except for waves of the longest periods, the gross features of Fig. 10 are determined mainly by the properties of the atmosphere below the elevations at which most of these factors become critical, and the curves can therefore be accepted in spite of these difficulties.

The group-velocity curves in Fig. 10 give information about the arrival times of waves of different periods. Phase-velocity curves can provide information

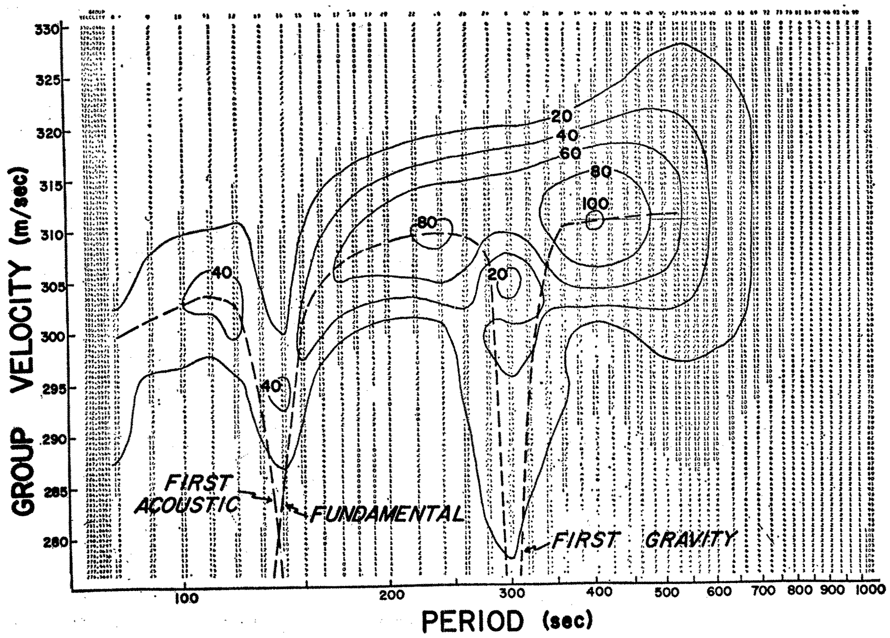


Fig. 11. Fourier analysis of a theoretical microbarogram and the group velocity curves (dashed lines) from which the microbarogram was derived. [After Pfeffer and Zarichny (*23*)]

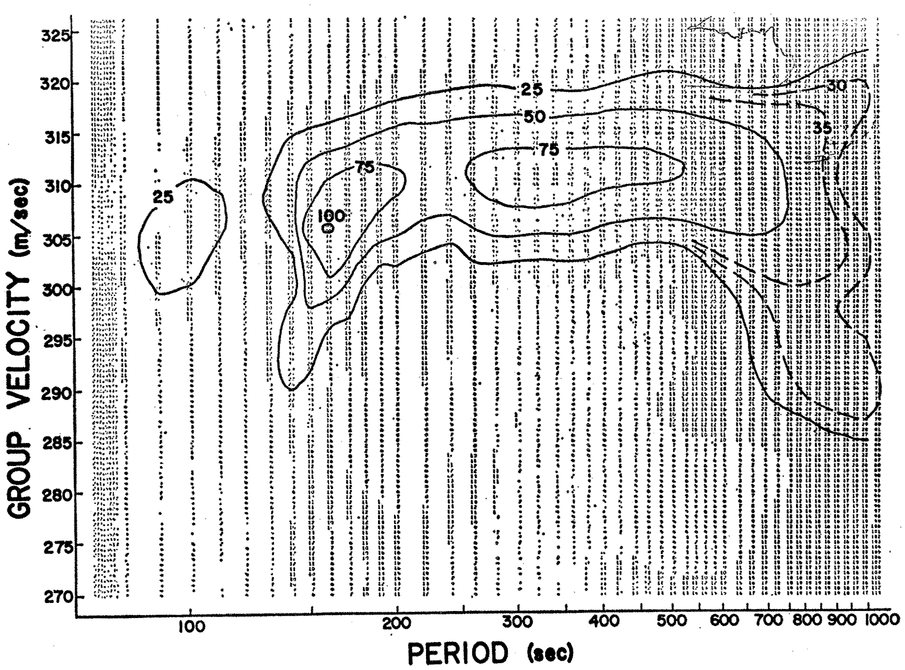


Fig 12. Fourier analysis of a Lamont Observatory microbarogram of 5 August 1962. [After Pfeffer and Zarichny (*23*)]

about the way in which the dispersion is controlled by the atmospheric structure. We consider here only the group velocity ($U$). Note that the quasi-horizontal portions of the group-velocity curves indicate a small change in velocity over a relatively broad period range. Within this range, a small packet of waves centered about a particular period should arrive nearly in phase and should thus produce large amplitudes. It would be expected, therefore, that the quasi-horizontal portions of the group-velocity curves, which occur in the range $290 < U < 315$ meters per second for the different modes, should be associated with wave arrivals of large amplitude. This is the range of velocities and periods that were obtained with the single-sound-channel atmospheres (Fig. 9), and the results lead to the conclusion that the longer-period waves should arrive first and should be followed by waves of successively shorter period; this is what is usually observed (Figs. 3 and 4).

There is a difference, however, between the dispersion curves based on the single-sound-channel atmosphere (Fig. 9) and those based on the two-channel atmosphere (Fig. 10): the latter indicate that the dispersion apparent on the wave records really consists of contributions from more than one mode of propagation and that there are small but distinct intervals of period separating the modes, at which little or no wave energy travels at a comparable speed.

### Spectrum Analysis of Wave Records

The fact that the intervals of period separating the horizontal portions of the different modes are so small explains the difficulty, noted earlier, in making satisfactory visual analyses of the wave spectra. To verify the existence of separate modes from pressure records at only one elevation requires a much finer frequency analysis of the records than can be made by visual measurement. It has been shown by Pfeffer and Zarichny (*23*) that this can be accomplished by taking the Fourier transform of portions of the wave record centered at successive times. In order to ascertain the dispersion relationships, these investigators plotted the pressure amplitudes on a chart as a function of both period and arrival time (or equivalently, group velocity) and drew contours of the field of amplitudes displayed in the velocity-period plane. Two examples, taken from their paper, are shown in Figs. 11 and 12. Figure 11 shows the results of testing the procedure with a known input consisting of a theoretical barogram derived from the velocity-period relationship shown by the dashed lines. The two-digit numbers are the actual computer output of Fourier amplitudes, normalized with respect to the largest amplitude in the field, and the solid lines are contours of this field. The individual modes are represented by the separate maxima in the amplitude field. Figure 12 gives the results of the analysis made by Pfeffer and Zarichny of the Lamont barogram of 5 August 1962 (shown in Fig. 3). The results show clearly the existence of three separate modes in the record.

Another, more rapid, method of making frequency analyses has been used successfully in the analysis of seismograms (*26*). This procedure involves the processing of data from an analog-computer tape by means of an electronic sound spectrograph. We have begun to apply this method to the analysis of pressure records from nuclear explosions. The procedure was tested for the input of Fig. 11 (shown in Fig. 13 by the continuous over-printed lines). The shaded region in Fig. 13 is the actual machine output, the density of the record is directly related to the amplitude of the signal. There seems to be good evidence, in the machine output, of the several modes shown in the input data, although the frequency resolution of the analysis obtained so far is not adequate to give perfect correspondence. Lack of perfect agreement between the spectrum analysis and the theoretical curves results from the poor time resolution in the spectrogram (from which velocities are computed) and also from the lack of uniformity of the analyzer in the period coordinate. The two types of data have slightly different frames of reference, which do not permit perfect matching.

Figure 14 is the spectrogram of the

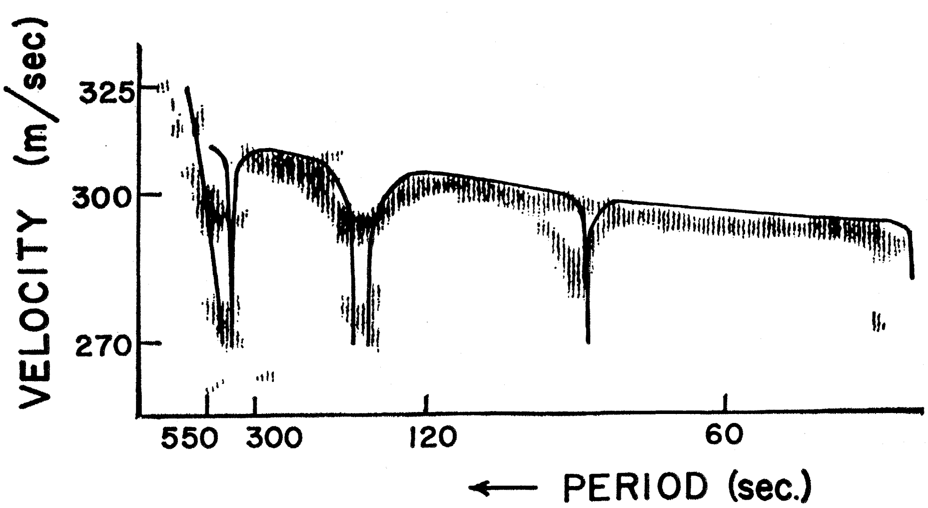


Fig. 13. Sound spectrogram of a theoretical microbarogram and the group velocity curves from which the microbarogram was computed.

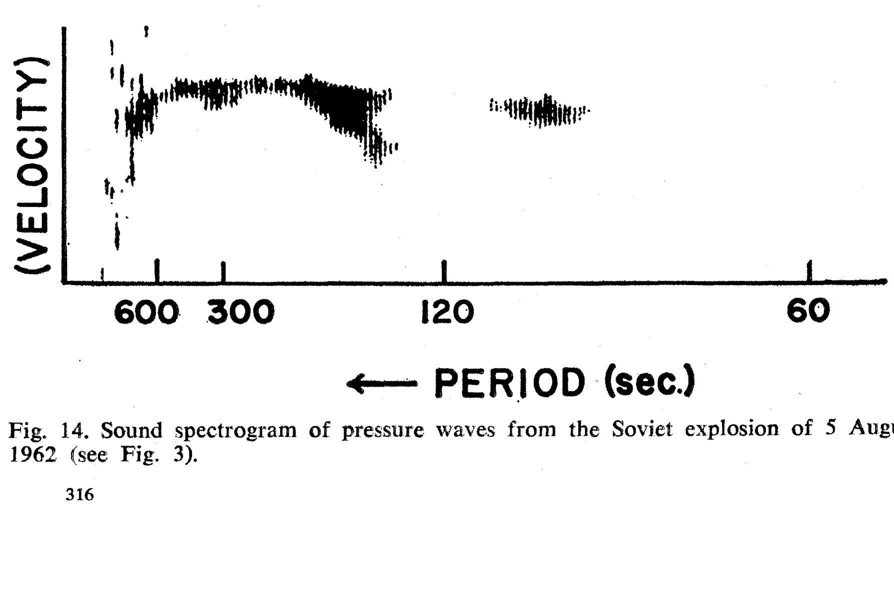


Fig. 14. Sound spectrogram of pressure waves from the Soviet explosion of 5 August 1962 (see Fig. 3).

Palisades record from the 5 August 1962 explosion in Novaya Zemlya (Fig. 3). The record indicates the existence of at least two modes separated by a break at a period of about 2 minutes. There is also evidence that the region from about 3 to 10 minutes involves more than one mode. Figures 12 and 14 also show a curvature at the long-period end which is suggestive of inverse dispersion in that an interpretation of decreasing velocity with increasing period could be given here.

### Critical Remarks

There is new evidence of inverse dispersion in certain of the records shown in Figs. 3 and 4, and in others not shown, as well as in the spectral analyses of Figs. 12 and 14. However, not all the barograms produced by a given explosion show this effect. Compare, for example, the Palisades and Honolulu barograms for the test of 5 August 1962; only the former shows inverse dispersion, although the amplitudes of the rest of the signal are equivalent in the two barograms. An examination of the cause of such differences should shed light on the origin of this effect. This can be studied by an analysis of (i) the temperature and wind structure of the atmosphere along the different paths, (ii) the elevation of the explosion, and (iii) the distance from the source. The possibility that the observed inverse dispersion is an apparent effect resulting from the superposition of different modes should also be examined.

We should also note that the frequency resolution of the spectral-analysis procedures decreases with increasing period. In order to gain further information about the number and types of modes present and the question of inverse dispersion at the longer periods, we are currently trying to obtain increased frequency resolution (*27*).

### References and Notes


1. G. Symond, Ed., *The Eruption of Krakatoa and Subsequent Phenomena* (Trubner, London, 1888).
2. F. Whipple, *Quart. J. Roy. Meteorol. Soc.* **56**, 287 (1930).
3. R. Yamamoto, *Meteorol. Res. Inst. Kyoto Univ. Meteorol. Notes, Ser. 2, No. 1* (1954), pp. 120–133.
4. W. Donn and M. Ewing, *J. Geophys. Res.* **67**, 1855 (1962).
5. ———, *J. Atmospheric Sci.* **19**, 264 (1962).
6. E. Carpenter, G. Harwood, and T. Whiteside, *Nature* **189**, 857 (1961); H. Wägner, R. Araskog, K. Edin, *Försvarets Forskningsanstalt* **1**, 32 (1962).
7. J. Brune, J. Nafe, L. Alsop, *Bull. Seismol. Soc. Am.* **51**, 247 (1961).
8. A discussion of the phase-velocity observations, now being accumulated from Soviet and United States tests of 1962, is in preparation.
9. M. Ewing and F. Press, *Bull. Seismol. Soc. Am.* **44**, 127 (1954).
10. R. Yamamoto, *Bull. Am. Meteorol. Soc.* **37**, 406 (1956).
11. R. Pfeffer and J. Zarichny, *J. Atmospheric Sci.* **19**, 256 (1962).
12. H. Lamb, *Hydrodynamics* (Cambridge Univ. Press, London, 1932).
13. H. Kallman-Bijl, R. Boyd, H. Lagow, S. Poloskov, W. Priester, *CIRA* (North-Holland, Amsterdam, 1961).
14. N. Sissenwine, M. Dubin, H. Wexler, *J. Geophys. Res.* **67**, 3627 (1962).
15. C. Pekeris, *Proc. Roy. Soc. London* **A171**, 434 (1939); *Phys. Rev.* **73**, 145 (1948).
16. R. Scorer, *Proc. Roy. Soc. London* **A201**, 137 (1950).
17. R. Yamamoto, *J. Meteorol. Soc. Japan* **35**, 288 (1957).
18. J. Hunt, R. Palmer, W. Penney, *Phil. Trans. Roy. Soc. London* **A252**, 275 (1960).
19. Y. Gazaryan, *Soviet J. Acoustics* **7** (July–Sept. 1961).
20. R. Pfeffer, *J. Atmospheric Sci.* **19**, 251 (1962).
21. V. H. Weston, *Can. J. Phys.* **40**, 431 (1962).
22. F. Press and D. Harkrider, *J. Geophys. Res.* **67**, 3889 (1962).
23. R. Pfeffer and J. Zarichny, *Geofis. Pura Appl.*, in press.
24. I. Harris and W. Priester, *NASA (Natl. Aeron. Space Admin.) Sci. Rept.* (1962).
25. This is not necessarily the case when we add to the problem the electromagnetic forces which must also come into play in the high atmosphere. See G. MacDonald, *J. Geophys. Res.* **66**, 3639 (1961).
26. M. Ewing, S. Mueller, M. Landisman, Y. Sato, *Geofis. Pura Appl.* **44**, 83 (1959).


27. This is Lamont Geological Observatory (Columbia University) contribution No. 590. We are grateful for the invaluable help of M. Landisman, J. Zarichny, and N. Balachandran in the analysis of wave records, and also grateful to J. Zarichny for his contributions to the mathematical analyses. This research was supported by the National Science Foundation (grants NSF-G-9412, NSF-GP-550, NSF-G-11997) and by the Office of Naval Research [contract Nonr 266(70)]. The theoretical calculations were performed on the IBM 7090 computer at the NASA Institute for Space Studies in New York City. We are indebted to the director, Dr. Robert Jastrow, for his kindness in making available the facilities of the Institute for this work.


**NEWS AND COMMENT**

# American Institute of Biological Sciences Accused of Misuse of NSF Grant Funds

The American Institute of Biological Sciences (AIBS) is in deep financial distress under circumstances that raise serious questions about its use of several hundred thousand dollars of government money.

The final accounting is yet to come. But the information so far available provides a disturbing view of unsanctioned use of grant funds. The bulk of these funds came from the National Science Foundation (NSF), which was largely responsible for transforming AIBS from a small organization into a $3-million-a-year concern, charged with administering a variety of NSF-funded projects. These ranged from a long-term multimillion dollar biology curriculum study to scientific meetings costing a few thousand dollars. Some of these were conceived by NSF and placed under AIBS administration; others, originating with AIBS, were proposed to the Foundation.

Along the way, in line with policies that have only recently been changed, NSF itself did not audit AIBS's records or inquire into its financial operations. When NSF, last fall, did become aware of AIBS's financial situation, it swiftly cut off further funds, pending a complete audit, and demanded that AIBS present a plan for repaying the government a shortage tentatively placed by NSF at $331,570. AIBS disputes the amount, although it concedes that a considerable amount is due.

In the meantime, under close NSF scrutiny, all but one of the projects entrusted to AIBS are continuing with

In this article, D. S. Greenberg of the *Science* staff describes the serious difficulties that face the American Institute of Biological Sciences and gives something of their history. In the following article, James D. Ebert, president of AIBS, discusses the responsibility of biologists to preserve AIBS.